Effects of Damage Accumulation on Quantum Well Intermixing by Low Energy Ion Implantation in Photonic Devices

M. Chicoine,[a] A. François,[b] C. Tavares,[b] S. Chevobbe,[b] F. Schiettekatte,[a] V. Aimez,[b] J. Beauvais,[b] and J. Beerens[b]

[a]Département de physique, Université de Montréal, Montréal (Qc), Canada
[b]Département de Génie Électrique et de Génie Informatique, Université de Sherbrooke, Sherbrooke (Qc), Canada

ABSTRACT

The surface layers of InP-based quantum well (QW) laser structures were implanted with As or P ions at energies ranging from 200 to 360 keV. The structures were then annealed at temperatures ranging from 650 to 750°C during 120 s, allowing the defects created by implantation to diffuse, resulting in intermixing at the barrier-QW interfaces. The consequence of the intermixing is the blue shift of the QW photoluminescence wavelength. The blue shift was studied as a function of the implantation temperature (25 or 200°C). Implantation-induced damage in the samples was characterized by Rutherford Backscattering in channeling mode (RBS-c) and correlated with the observed blue shift. It is found that blue shift is more efficient at higher implantation temperature, even if the resulting defect concentration is much lower. This is attributed to the diffusion of defects during high-temperature implantation, leading to a larger region containing defects contributing to intermixing. Also, when the implanted dose is too high, no blue shift is observed. This could be due to the formation of defect clusters that inhibits the subsequent diffusion of defects. Finally the defect creation mechanisms within InP and InGaAs layers are found to have a significant impact on the resulting wavelength blue shift.

Keywords: Quantum well intermixing, Low energy ion implantation, RBS, Photoluminescence

1. INTRODUCTION

Wavelength division multiplexing (WDM) increases the optical fiber bandwidth by multiplying the number of available wavelengths that can be handled simultaneously. Such systems are based on either tunable lasers or by the combination of several discrete single-wavelength devices. Multiple wavelength integration on a single photonic device would allow a significant improvement of the performance and costs associated with multiplexing. It would also enable a much higher degree of interoperability between the different channels, allowing important developments for future generation photonic networks.[1] The technical difficulty associated to such components arises from the difficulty of integrating multiple bandgaps on the same device. Indeed, semiconductor lasers and modulators are based on Quantum Well (QW) structures fabricated by epitaxial growth. As illustrated in Fig. 1, multi-wavelength lasers require several single-wavelength lasers, which implies structures with different bandgap values; electro-optic modulators also require bandgap tuned semi-absorbing regions for quantum confined Stark effect and finally, integration of low absorption waveguides involves even higher bandgap tuned regions. Currently, in order to fabricate these structures, techniques such as selective area epitaxy[2] and etching and regrowth[3] are used but these methods require several cycles of epitaxial growth in order to create the different components, meaning high costs and limited throughput.

An attractive alternative is to use ion implantation induced Quantum Well Intermixing (QWI).[4–8] With this technique, structural defects created by ion implantation can be positioned in the near-surface region i.e. far away from the active region. Indeed, with InP based structures, the defect diffusion can be sufficiently efficient to allow a large separation

Further author information: (Send correspondence to F. Schiettekatte or V. Aimez)
F. Schiettekatte: E-mail: francois.schiettekatte@umontreal.ca, Telephone: (514) 343-6049, Address: Laboratoire René-J.-A.-Lévesque, 2905 Chemin des Services, Université de Montréal, Montréal, Québec, Canada H3T 1J4
V. Aimez: E-mail: vincent.aimez@usherbrooke.ca, Telephone: (819) 821-8000 ext. 2137, Address: Electrical Engineering dept., Université de Sherbrooke, Sherbrooke, Québec, Canada J1K 2R1

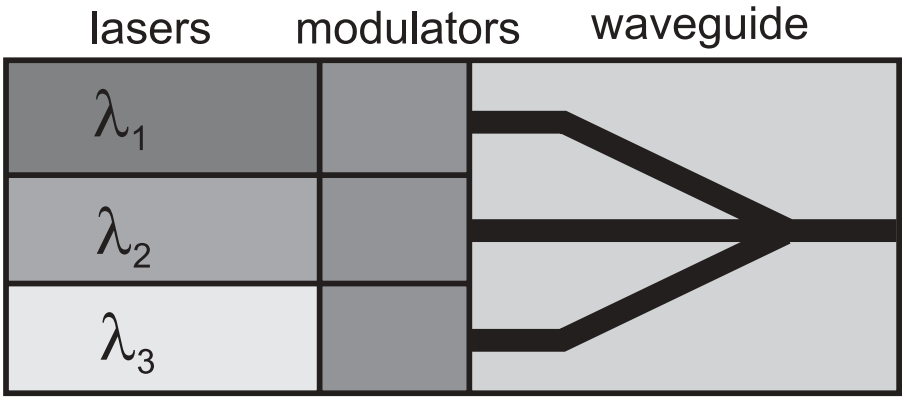

Figure 1. Schematic representation of an integrated photonic device. Each laser has a different wavelength; the modulator bandgaps have to be adjusted so that they are semi-absorbing at their corresponding laser wavelength; the waveguide bandgap must be high enough to achieve low absorption.

between the ion implanted layers and the quantum well region; furthermore, it has been also demonstrated that there is a close relationship between the amount of defects created controlled by varying the dose and the resulting blue shift obtained.[9] When the structure is thermally annealed, the defects diffuse and induce intermixing. The effect of inter-diffusion at QW interfaces is to smooth the shape of the wells which results in a bandgap increase thus a blue-shifted emission wavelength. Selected areas of a device can thus be implanted at specific doses in order to provide the amount of blue shift required by the different regions of an integrated photonic device. It has been shown with aging tests that shallow implantation induced QWI can be used to produce high-reliability blue-shifted lasers.[8]

In the case of InP-based QW structures, low energy implantations are typically carried out with $200-400$ keV P or As ions. The blue shift first increases with implanted dose and eventually saturates at $\approx 1\times10^{14}$ ions/cm^2. Increasing the dose then deteriorates device quality. The blue shift also increases with implantation temperature, until it saturates at $\approx 200^{\circ}$C. A maximum of $\approx 100-120$ nm blue shift is typically obtained for As doses of the order of 1×10^{14} at/cm^2 and implantation temperatures of 200°C, followed by a 650°C annealing. Since low ion energies are used, the secondary defects created by implantation are situated far from the active region of the device and do not affect the performance of the device.

These dose and temperature dependencies suggest a relatively complex role played by the defect generation and subsequent diffusion. Although ion implantation-induced QWI has been studied in details for specific structures, the relation between the amount and type of damage created by implantation and the observed blue shift is not fully understood. In order to identify the fundamentals of the damage process, relating information on the actual defect distribution after implantation and its relation with implantation temperature is of prime importance. In this work, we use Rutherford Backscattering Spectrometry in channeling mode (RBS-c) to measure the defect profiles obtained after Room Temperature (RT) and 200°C implantations of 200 keV As or P ions in standard InGaAs/InGaAsP QW laser structures. They are compared to the photoluminescence (PL) for these samples and results obtained form other experiments.

It is found that both the implantation temperature and the layer in which the ions are implanted have a significant effect on the intermixing efficiency. Any damage accumulation in the InP cladding of a device significantly impedes intermixing, as if such damaged layer blocked point defect release or diffusion. When the temperature is high enough to prevent quick amorphization of the InP, or when a sacrificial InP layer is added on the top of the InGaAs contact layer in order to stop the 200 keV As ions before they reach the InP cladding, or if lower energies (30 keV) are used so the ions do not reach the cladding, much better blue-shifts are obtained. As it will be discussed, this confirms that direct damage produced in the cladding can inhibit defect diffusion.

2. EXPERIMENTAL DETAILS

Two epitaxial structures were used for these experiments. Firstly, a lattice-matched 5 QW laser structure (identified as ITME2415 in this text) has been grown by MOCVD on an InP(100) sulfur-doped substrate at the Institute of Electronic

Materials Technology (ITME) in Warsaw, Poland. The structure is schematically shown in Fig. 2. The active region of the laser consists of 5 InGaAs quantum wells with 12 nm InGaAsP barriers. The structure is capped by a 200 nm thick undoped InP layer on top of the InGaAs contact layer. The room temperature emission wavelength of this structure is centered at 1.54 μm. Some of the samples had the top InP layer chemically etched before implantation. A more simple undoped structure (identified as RII in this text) that had only one 5 nm quantum well with 20 nm InGaAsP barriers, grown by CBE at NRC was also used for some experiments.

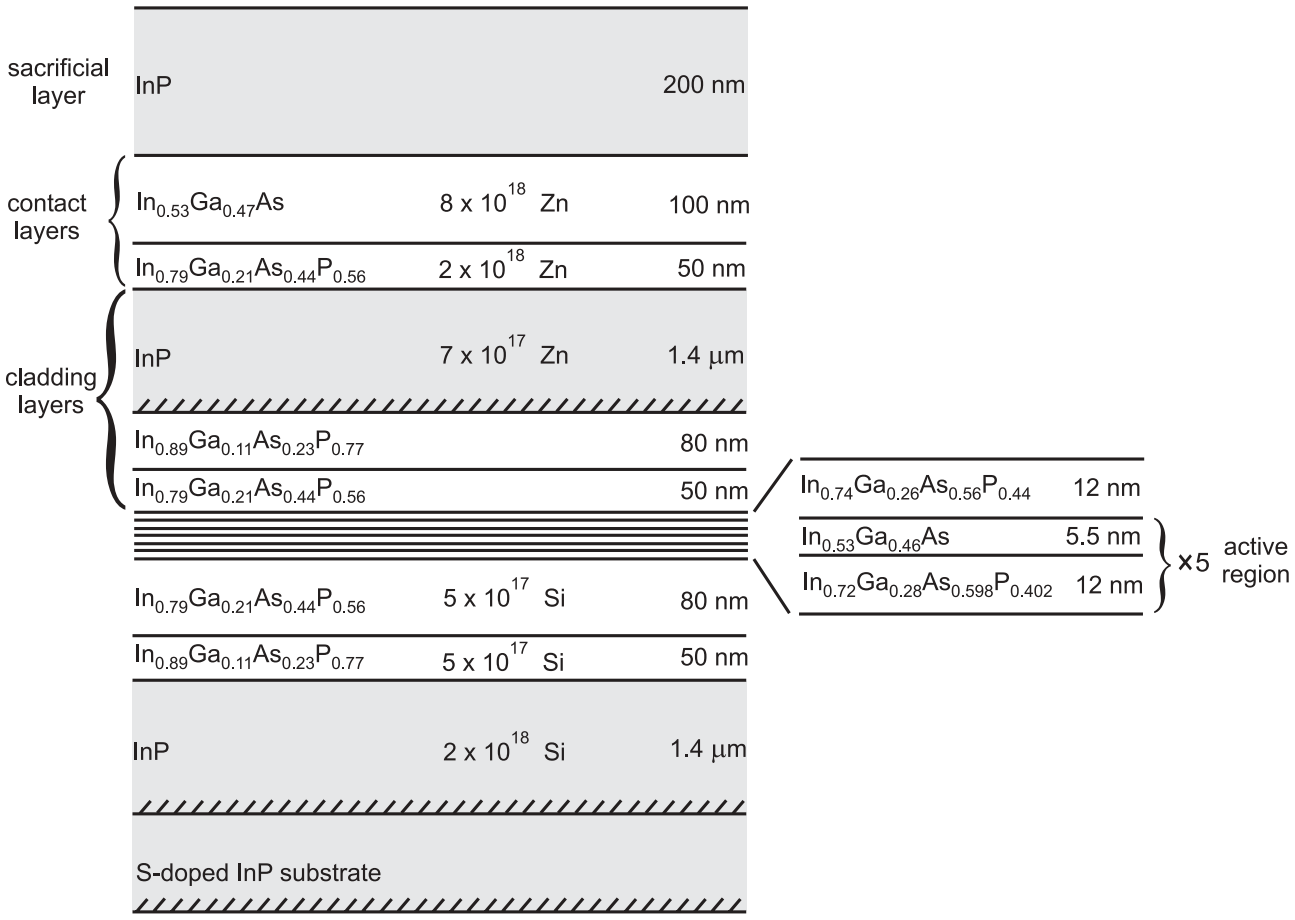

Figure 2. Schematic representation of the laser structure used in this work. Doping is indicated in the central column in cm^{-3} units. The InP layers are grey-shaded for clarity.

These heterostructures have been implanted either by phosphorus or arsenic ions with energies ranging from 200 to 360 keV, with doses ranging from of 200 to 360 keV, at doses ranging from 1.5×10^{13} to 1×10^{14} at/cm^2. The implantation temperature was either 25 or 200°C. The implantations have been carried out either on the 200 kV Varian DF-3000 implanter at the Université de Sherbrooke or on the 1.7 MV Tandetron accelerator at the Université de Montréal. The angle of incidence on the target was set to 7° to minimize channeling. The implanted samples were then annealed in a Rapid Thermal Annealing (RTA) furnace at temperatures ranging from 650 to 700°C during 120s. The surface of the samples was covered by a piece of InP material during annealing in order to minimize surface degradation.

Photoluminescence was carried out at 16 K using a 905 nm laser diode and recorded with a germanium detector cooled with liquid nitrogen. The signal was chopped at 400 Hz and passed through a lock-in amplifier and a spectrometer with a focal length of 500 mm. The defect profiles were obtained from RBS-c measurements on the Tandetron accelerator using either 2 or 3 MeV He+ beams. The channeling direction was found with a precision better than 0.1° by interpolating between planar channeling directions.

3. RESULTS

3.1. Photoluminescence

Photoluminescence was measured for ITME2415 samples implanted at 200°C with 1×10^{14} As/cm^2 ions at 300 keV and annealed at 680°C for 120 s. A set of samples had the InP sacrificial layer etched before implantation. The implanted ions profiles for samples with (type A) and without (type B) the InP sacrificial layer are shown schematically in Fig. 3. This figure shows that, in the case of a sample with an InP sacrificial layer (type A), the ions are stopped in the InGaAs contact layer and do not reach the InP cladding layer while they reach this layer when the sacrificial layer is etched (type B). Fig. 4 shows the PL spectra from an as-grown sample (a), an annealed sample for control (b), a type B sample implanted and annealed (c), a type A sample implanted and annealed (d), and same sample as (d), after its InP sacrificial layer was etched (e). The annealed control sample is thermally blue-shifted by 6 nm and its intensity is $\approx 25\%$ higher than the as-grown sample. The PL intensities from annealed as-grown samples are usually $\approx 5-10\%$ higher than from unannealed as-grown samples. The results for the implanted samples are summarized in Table 1.

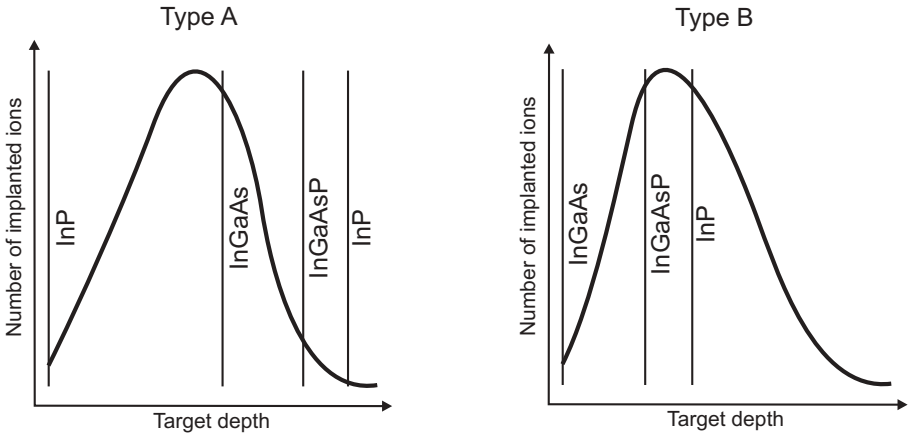

Figure 3. Schematic representation of the number of implanted 300 keV As ions as a function of depth in samples with (type A) and without (type B) the InP sacrificial layer

The indicated blue shifts and relative intensities are measured relatively to the unimplanted control sample that was annealed at the same time. It is shown that the largest blue shift is obtained for samples with the InP sacrificial layer and that the intensity and wavelength blue shift is significantly lower for samples that had this layer etched before ion implantation. As it will be seen in the next sections, these results illustrate the fact that damage produced in the InP cladding layer decreases the efficiency of intermixing. Also, as seen with sample (e), the effect of etching the InP sacrificial layer after the anneal is to bring back the PL intensity from 30% to $\approx 90\%$ of the as-grown sample intensity. This shows that damage in InP strongly absorbs the PL signal. This sample also has a FWHM of 20 nm, which is significantly lower than a FWHM of 30 nm for the as-grown sample. Therefore, structures with an InP sacrificial layer offers many advantages in terms of blue shift, PL signal quality while significantly lowering the remaining damage accumulation in the resulting sample, all such aspects playing a significant role for potential industrial applications.

PL was also measured for samples with structure RII implanted with 1×10^{14} As/cm^2 at 200 keV and annealed at 700°C for 120 s. The implantation temperature was either 25 or 200°C and some samples had the top InGaAs layer (contact layer) etched. These results are summarized in Table 2. The PL intensity from implanted samples was about 50% of the intensity of reference samples. It is seen that the largest blue shift is obtained for the sample implanted at 200°C in the InGaAs contact layer and that no significant blue shift is obtained for heavily damaged samples, especially when the implantation is carried out directly in the InP cladding layer. The amount of damage is estimated from RBS-c measurements, as it will be discussed in the next section.

3.2. Damage profiles

RBS-c was used to investigate the damage profiles from as-implanted samples. The middle curve of Fig. 5 shows the RBS-c profiles of a RII sample that was implanted at room temperature with 1×10^{14} As/cm^2 at 200 keV. For comparison, spectra

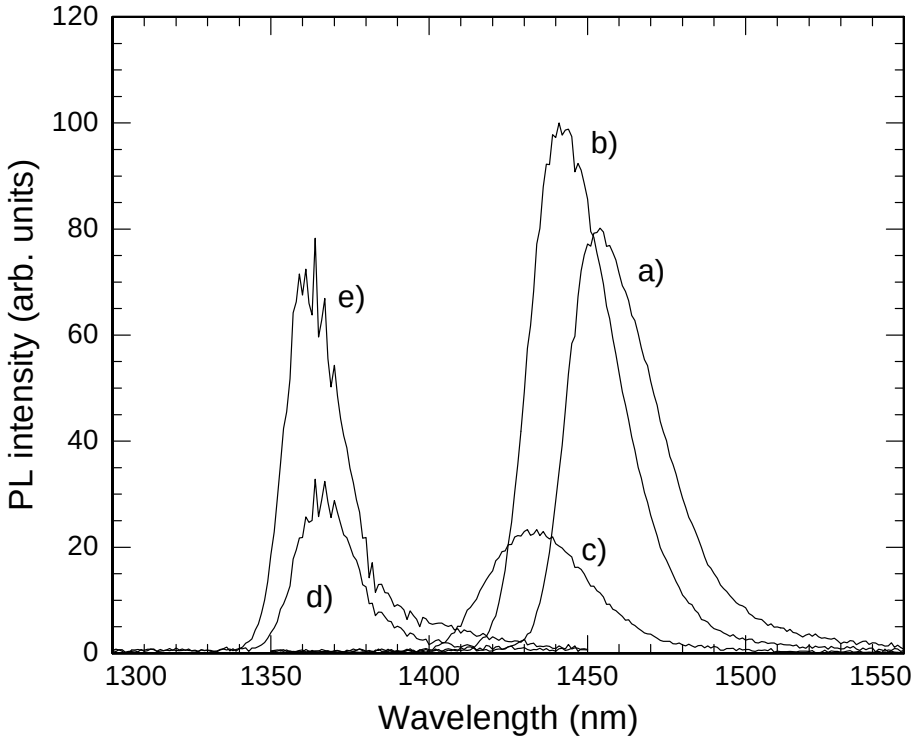

Figure 4. PL spectra for an ITME2415 type A sample a) as-grown, b) annealed, c) type B implanted and annealed, d) type A implanted and annealed, and e) same sample as d) with InP sacrificial layer etched after annealing.

Table 1. Summary of implanted samples PL blue shifts relative to the control sample. PL intensity is relative to the as-grown sample.

Sample	PL shift	Intensity	FWHM
c) (type B)	8 nm	20%	30 nm
d) (type A)	80 nm	30%	20 nm
e) (type A)*	88 nm	90%	22 nm

* Same sample as c), after etching the InP sacrificial layer.

Table 2. Summary of PL blue shift and measured damage for samples with structure RII. Damage is measured by RBS-c and expressed in In interstitial concentration.

Impl. temp.	Top layer	PL shift	Damage
25°C	InGaAs contact layer	34 nm	13 at.%
200°C	InGaAs contact layer	116 nm	no observable damage
25°C	InP cladding layer	no shift	heavy damage
200°C	InP cladding layer	no shift	heavy damage

from an as-grown RII sample in channeling (bottom curve) and random (top curve) orientations are shown. The curve from a sample that was implanted at 200°C, which is not presented in this figure, showed no difference from the as-grown sample. The spectra were acquired with a 3 MeV He+ beam. The thick line represents the In interstitial concentration, which was extracted from the RBS-c profile with the ALEGRIA program.[10] It reaches up to 13% of In interstitial concentration. It can be seen that this curve has two maxima. The first one located in the InGaAs layer at about 75 nm, corresponding to the average depth of the In interstitials, as calculated with the TRIM code.[11] The second maximum is located in the InP layer. The existence of this second peak reflects the fact that InP is more sensible to radiation damage than InGaAs. Even if a small number of As ions end up in the InP layer, each ion creates a significantly higher amount of interstitial in InP than in InGaAs, resulting in an increase of the measured damage.

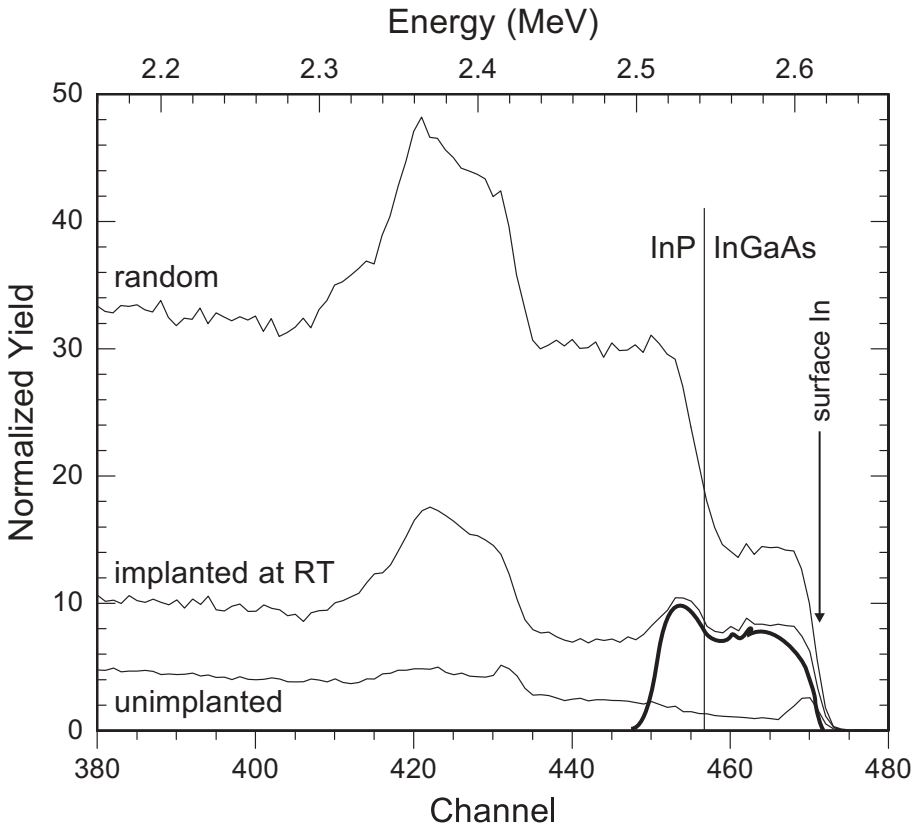

Figure 5. RBS-channeling spectra from a sample implanted at room temperature with 1×10^{14} As/cm^2 at 200 keV. The vertical line indicates the position of the InGaAs/InP interface for the In signal. The arrow indicates the position of the surface In signal. The thick line represents In interstitial concentration. Spectra from an as-grown sample in channeled (bottom curve) and random (top curve) directions are shown for comparison.

The fact that InP is much more sensitive to irradiation damage than InGaAs can also be verified on Fig. 6. The RBS-c spectra shown in this figure were taken from samples for which the InGaAs contact layer was etched before implantation, this time with a 2 MeV He+ beam. They were implanted with the same ion dose and beam energy as the samples in Fig. 5. It is seen that the sample implanted at room temperature is heavily damaged as the near-surface region of the spectrum reaches the same level as the spectrum from a randomly oriented sample. By contrast, the sample implanted at 200°C is less damaged and over a smaller region. This reduction in resulting damage for samples irradiated at 200°C is due to dynamic annealing during implantation.

The threshold for damage detection by the RBS-c technique was also investigated. Fig. 7 shows RBS-c spectra from InGaAs-stripped samples implanted at 200°C with 200 keV P ions. The implantation doses are indicated on the figure. The spectrum from an unimplanted sample (bottom curve) is shown for comparison. While no additional features are observed

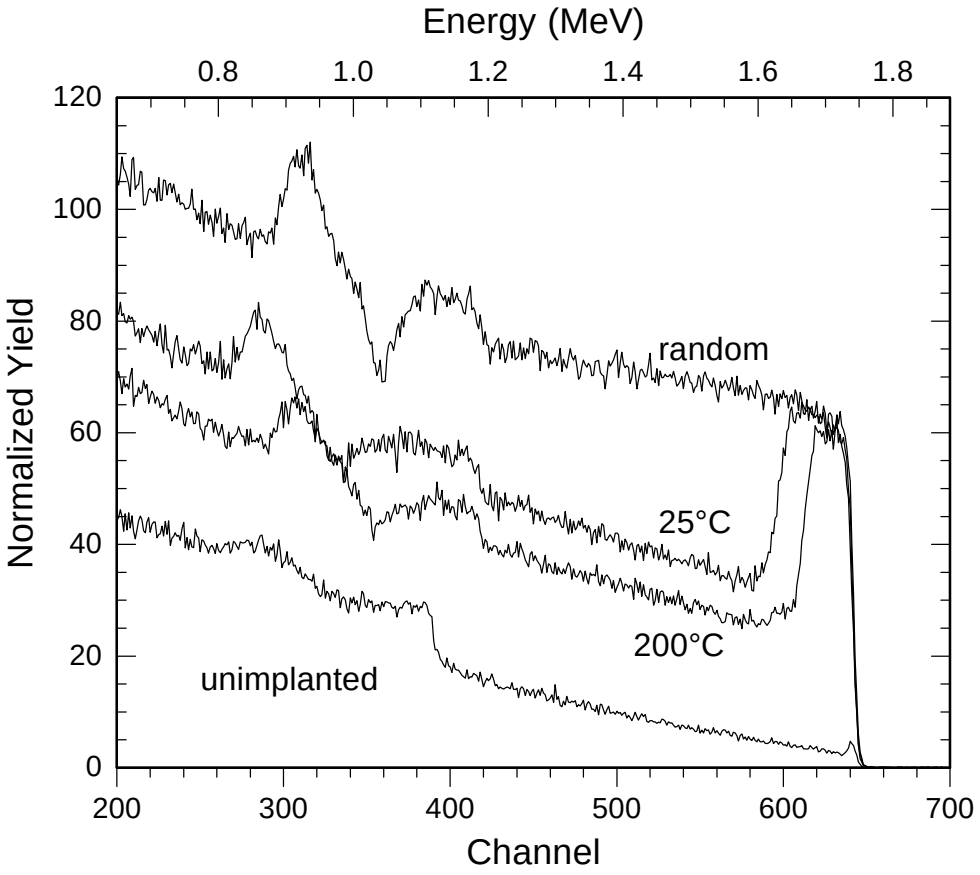

Figure 6. RBS-channeling spectra for samples directly implanted at RT in InP (the InGaAs contact layer was etched before implantation) with 1×10^{14} As/cm^2 at 200 keV. Spectra from an unimplanted sample in channeled (bottom curve) and random (top curve) are shown for comparison.

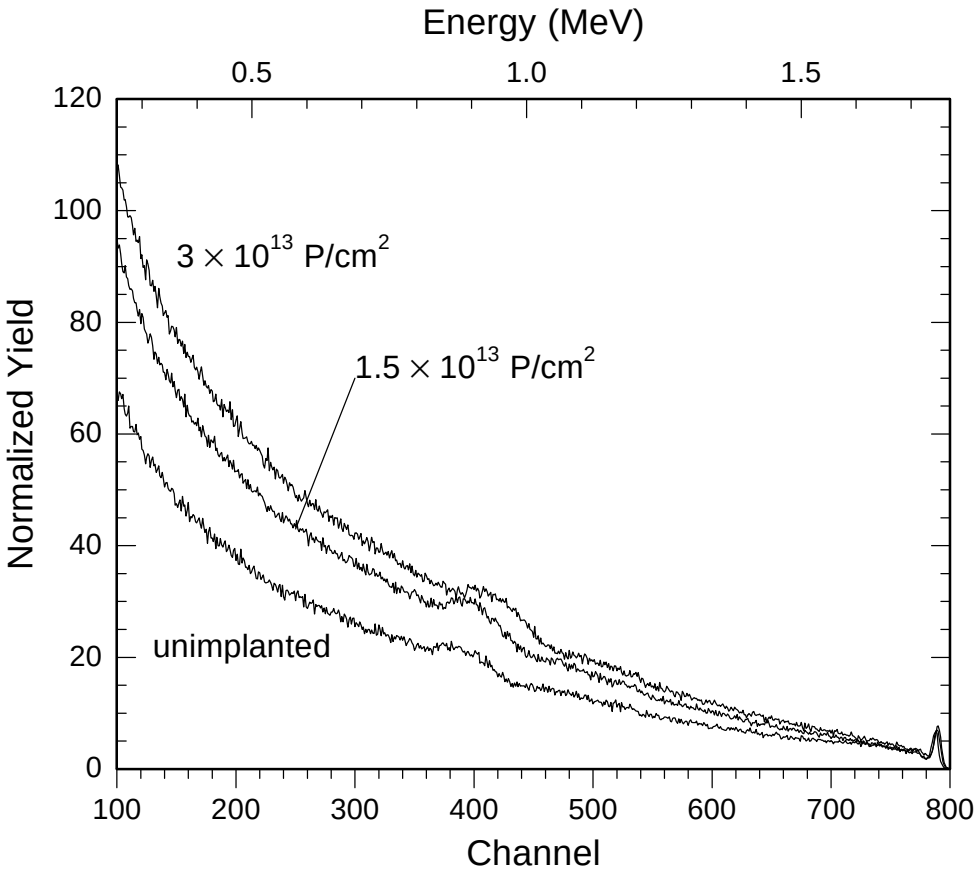

Figure 7. RBS-channeling spectra for samples directly implanted at 200°C in InP (the InGaAs contact layer was etched before implantation) with 200 keV P ions.

on the implanted samples spectra, it is seen that the overall intensity is higher at lower backscattered He energies. This is indicative of residual damage that is either in the implantation region or that could have diffused deeper in the sample.

4. DISCUSSION

It was found that for the ion dose range that leads to interesting PL shifts in structure RII, damage is only detectable by RBS-c as low energy dechanneling and that this dechanneling increases with ion dose, as seen in Fig. 7. This, combined with the fact that higher implantation temperatures lead to larger blue shifts, could also indicate that at high implantation temperature, some of the defects have already diffused in the material *during* the implantation, allowing to keep a defect concentration that is locally lower but distributed over a larger region, allowing a larger total number of defects to be in a state in which they can contribute to QW intermixing.

Increasing the ion dose then leads to localized damage profiles detectable by RBS-c, but with reduced PL shifts. Carmody *et al.*[12] recently found similar results in terms of InP amorphization after RT implants in the InP cladding, and concluded that RT implants in InP produce more stable cluster that will not contribute as much to the intermixing compared to 200°C implants. The implantation doses in an InGaAs contact layer were not sufficient to reach intermixing saturation. As for our results, their InP results imply that the concentration of defects must be low enough so that they are in a state where they can be easily released upon thermal annealing and contribute to QW intermixing. Moreover, as suggested from Fig. 3 and the results of table 1, when there is a damaged InP region between the projected range of the ions and the quantum wells, PL blue shift is reduced. We propose the following explanation. As it has been discussed in section 3.2, InP is much more sensible to damage than InGaAs so that the ions that reach the InP cladding layer as seen in Fig. 3 will

create a large amount of damage. Then this highly damaged layer acts as a diffusion barrier for the intermixing-related defects during subsequent annealing.

5. CONCLUSION

In conclusion, we have shown that the reduction of PL blue shift for samples implanted at high ion doses is related to damage accumulation that inhibits defect diffusion upon thermal annealing. It was also suggested that high-temperature implantations lead to more efficient QW intermixing because defect diffusion occurs during ion implantation. This allows to distribute the intermixing-related defects over a larger region while keeping their concentration low enough so that a larger number of defects are available for intermixing.

ACKNOWLEDGMENTS

The authors are grateful to Réal Gosselin, Louis Godbout and P. Lafrance for their technical assistance, as well as P. Poole from NRC (Ottawa, Canada) for CBE growth. This work benefited of grants from the NSERC of Canada and FCAR of Québec.

REFERENCES

1. E. Modiano, "Traffic grooming in WDM networks," *IEEE Commun. Mag.* **39**, p. 124, 2001.
2. D. Delprat, A. Ramdane, L. Silvestre, A. Ougazzaden, F. Delorme, and S. Slempkes *IEEE Photon. Technol. Lett.* **9**, p. 898, 1997.
3. P. I. Kuindersma, P. P. G. Mols, G. L. A. v. d. Hosfad, G. Cuypers, M. Tomesen, T. V. Dongen, and J. J. M. Binsma *Electron. Lett.* **29**, p. 1876, 1993.
4. V. Aimez, J. Beauvais, J. Beerens, D. Morris, H. Lim, and B. Ooi *J. Selected Topics in Quantum Electronics* **8**, p. 870, 2002.
5. S. Charbonneau, P. J. Poole, Y. Feng, G. C. Aers, M. Dion, M. Davies, R. D. Goldberg, and I. V. Mitchell *Appl. Phys. Lett* **67**, p. 20, 1995.
6. M. Paquette, V. Aimez, J. Beauvais, J. Beerens, P. J. Poole, S. Charbonneau, and A. P. Roth *J. Selected Topics in Quantum Electronics* **4**, p. 741, 1998.
7. H. J. Chen, H. A. McKay, R. M. Feenstra, G. C. Aers, P. J. Poole, R. L. Williams, S. Charbonneau, P. G. Piva, T. W. Simpson, and I. V. Mitchell *J. Appl. Phys.* **89**, p. 4815, 2001.
8. J.-P. Noël, D. Melville, T. Jones, F. Shepherd, C. J. Miner, N. Puetz, K. Fox, P. J. Poole, Y. Feng, E. S. Koteles, S. Charbonneau, R. D. Goldberg, and I. V. Mitchell *Appl. Phys. Lett.* **69**, p. 23, 1996.
9. P. J. Poole, S. Charbonneau, G. C. Aers, T. E. Jackman, M. Buchanan, M. Dion, R. D. Goldberg, and I. V. Mitchell *J. Appl. Phys.* **78**, p. 2367, 1995.
10. F. Schiettekatte and G. Ross in *Proceedings of the 14th International Conference on the Application of Accelerators in Research and Industry* (Denton, USA), AIP Press, 1996.
11. J. F. Ziegler, J. P. Biersack, and U. Littmark, *The Stopping and Range of Ions in Solids*, Pergamon Press, New York, 1985.
12. C. Carmody, H. H. Tan, and C. Jagadish *J. Appl. Phys.* **93**, p. 4468, 2003.